ELSEVIER

Earth and Planetary Science Letters 186 (2001) 1–6

EPSL

www.elsevier.com/locate/epsl

Express Letter

# Radial variations of melt viscosity around growing bubbles and gas overpressure in vesiculating magmas

Nadav G. Lensky *, Vladimir Lyakhovsky, Oded Navon

*Institute of Earth Sciences, The Hebrew University, Jerusalem 91904, Israel*

Received 16 October 2000; accepted 3 January 2001

**Abstract**

The viscosity of silicic melts depends strongly on their water content. As bubbles grow in a supersaturated melt, water evaporates from the bubble–melt interface. A diffusive profile develops and leads to steep viscosity gradients across the melt shell. Here we investigate the effects of radial viscosity profiles on the dynamics of bubble growth. We find that the effective melt viscosity resisting gas overpressure in the bubbles is close to the viscosity at the dehydrated rind, and may be higher than that of the surrounding melt by more than an order of magnitude. As a result, bubbles may retain pressures that are higher than ambient pressure for longer times, magma degassing is delayed to shallower depth, and fragmentation of magma due to gas overpressure may occur over a wider range of conditions. Measured water content in eruption products yields information on the average melt viscosity, however additional information about the concentration profiles is needed for estimating the effective viscosity that controlled the evolution of bubble growth in the ejecta. 

*Keywords:* viscosity; bubbles; magmas; pressure

## 1. Introduction

The diversity of volcanic eruptions is widely attributed to the extreme range of viscosities of the erupting magma [1]. During an eruption, as highly viscous silicic magma ascends and decompresses, its dissolved volatiles become supersaturated and gas bubbles nucleate and grow. Gas overpressure in the bubbles is maintained by falling ambient pressure, continuous exsolution of the volatiles, and the viscous resistance of the melt around the bubbles. At high ascent rates, when the strength of the melt is exceeded either by gas overpressure in the bubbles [2–4] or by high strain rates of the flow [5,6], the bubble-bearing magma fragments and erupts explosively [7,8].

The gas overpressure in the bubbles is supported by viscous stresses in the surrounding melt. When melt viscosity is uniform, gas overpressure is proportional to the viscosity of the melt; high-viscosity melts preserve higher overpressures and are more likely to fragment. However, over a wide range of volcanic conditions, narrow rinds of highly viscous melt develop around the growing bubbles due to dehydration of the melt. This effect of variable melt viscosity

* Corresponding author. Tel: +972-2-658-6513; Fax: +972-2-566-2581; E-mail: nadavl@vms.huji.ac.il

0012-821X/01/$ – see front matter 
PII: S0012-821X(01)00227-8

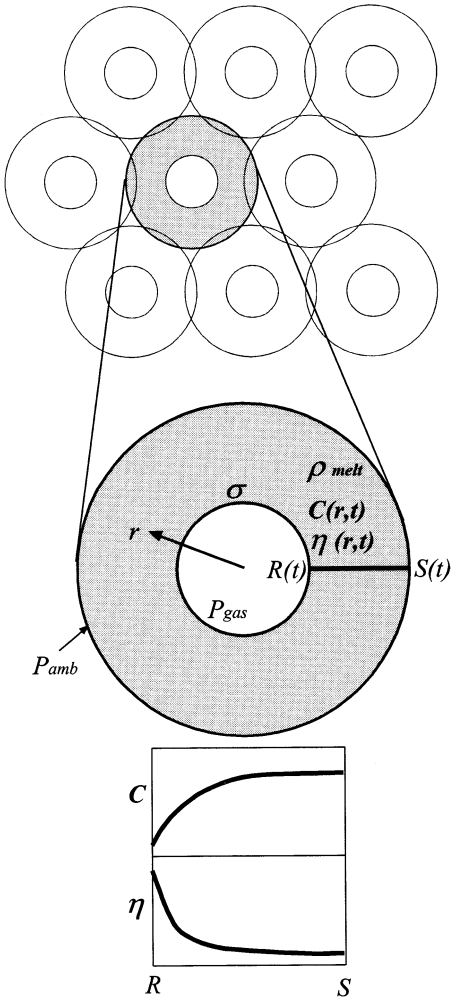


Fig. 1. Magma is regarded as a pack of spherical cells, each composed of a gas bubble with radius $R$ centered in a spherical melt shell with outer radius $S$. The cells are uniform in size and arranged in a three-dimensional lattice so that the gas volume fraction of the magma is $(R/S)^3$. The melt shell is incompressible and viscous and contains dissolved oversaturated water. The diffusive transfer of water results in a concentration profile, typically $C \propto 1/r$, during the quasi-static stage, and to a corresponding viscosity profile [12].

has been incorporated in numerical simulations of bubble growth [9,10], but has not been thoroughly analyzed.

In this study we explore the effects of radial variations of melt viscosity on the growth of bubbles. We analyze the hydrodynamic equations of the melt around a bubble and demonstrate that the effective viscosity is strongly dictated by the high-viscosity rind that forms at the bubble–melt interface.

## 2. The hydrodynamics of the melt around a growing bubble

The growth of gas bubbles is driven by gas overpressure and resisted by the viscous melt around the bubble. Following the physical model of Proussevitch and Sahagian [10], we consider magma as a suspension of spherical gas bubbles that do not interact with each other. We assume uniform bubble radii and a uniform bubble distribution so that a spherical cell consisting of a single bubble and the surrounding melt shell represents the whole magma (Fig. 1). Considering the equation of fluid motion and equation of continuity, we solve for the viscous resistance of the melt around the growing bubble.

The Navier–Stokes equation of motion for the spherically symmetric melt shell, neglecting inertial terms, is [11]:

$$0 = -\frac{\partial P}{\partial r} + \frac{\partial \tau_{rr}}{\partial r} + \frac{2}{r}\tau_{rr} - \frac{1}{r}(\tau_{\phi\phi} + \tau_{\theta\theta}) \qquad (1)$$

where $P$ is pressure and $\tau_{rr}$, $\tau_{\phi\phi}$ and $\tau_{\theta\theta}$ are the radial and tangential components of the deviatoric stress tensor. For a Newtonian fluid with viscosity $\eta$, these components are [11]:

$$\tau_{rr} = 2\eta\frac{\partial v_r}{\partial r}, \qquad \tau_{\phi\phi} = \tau_{\theta\theta} = 2\eta\frac{v_r}{r}. \qquad (2)$$

The melt velocity, $v_r$, around a growing bubble of radius $R$ with radial growth velocity $\dot{R}$ is obtained by integrating the equation of continuity for the incompressible melt:

$$v_r = \dot{R}R^2\frac{1}{r^2} \qquad (3)$$

Substituting Eq. 3 into Eq. 2 and then into Eq. 3 yields:

$$\frac{\partial P}{\partial r} = -4\dot{R}R^2\frac{1}{r^3}\frac{\partial \eta}{\partial r} \qquad (4)$$

The boundary condition at the bubble–melt interface is obtained by equating the total stress

with the difference between the gas pressure, $P_{gas}$, and the Laplace surface tension ($2\sigma/R$):

$$(-P+\tau_{rr})|_R = -P_{gas}+2\frac{\sigma}{R} \quad (5)$$

At the outer boundary of the melt shell, the total stress is set equal to the ambient pressure, $P_{amb}$:

$$(-P+\tau_{rr})|_S = -P_{amb} \quad (6)$$

Integrating Eq. 4 with boundary conditions (Eqs. 5 and 6) yields the mechanical equilibrium condition between viscous stresses in the melt shell and gas overpressure in the bubble:

$$P_{gas}-P_{amb}-\frac{2\sigma}{R}=4\frac{\dot{R}}{R}\eta_{eff} \quad (7)$$

where the effective viscosity, $\eta_{eff}$, may be written in two forms:

$$\eta_{eff}=\eta_R\left[1-\frac{\eta_S}{\eta_R}\left(\frac{R}{S}\right)^3+\frac{R^3}{\eta_R}\int_R^S\frac{d\eta}{dr}\frac{1}{r^3}dr\right]=$$

$$3R^3\int_R^S\frac{\eta(r)}{r^4}dr \quad (8)$$

where $\eta_R$ and $\eta_S$ are the viscosities at the two shell boundaries. In the following section we discuss the values of effective viscosity relative to $\eta_R$ and to $\eta_S$ during dehydration of the melt shell.

## 3. Effective viscosity of a dehydrating melt shell

As bubbles grow in a supersaturated melt, water evaporates from the bubble–melt interface and a diffusive profile develops. The strong dependence of melt viscosity on water concentration [12] leads to extreme viscosity gradients across the melt shell. To obtain an analytical expression for the effective viscosity (Eq. 8) we approximate the radial viscosity distribution, $\eta(r)$, by a general power law of the non-dimensional distance ($r/R$):

$$\eta(r)=\eta_R\left[1-\left(1-\frac{\eta_S}{\eta_R}\right)\frac{\left(\frac{r}{R}\right)^n-1}{\left(\frac{S}{R}\right)^n-1}\right] \quad (9)$$

When the power parameter $n$ is 1, the viscosity profile is linear. The steeper gradients achieved during dehydration require smaller values of $n$ (for $n=0$, the last fraction in the square brackets should be replaced by $\ln(r/R)/\ln(S/R)$). For example, the viscosity profile around a quasi-statically growing bubble [13] in a rhyolitic melt with water concentrations of $C_R=0.1$ wt% and $C_S=0.6$ wt% is bounded by Eq. 9 with $n=-3$ and $n=-9$ (Fig. 2a). Transient water diffusion and/or variable water diffusivity [14] will lead to steeper concentration profiles and thus to steeper viscosity profiles (smaller $n$). Substituting Eq. 9 into Eq. 8 yields the effective viscosity:

$$\eta_{eff}=$$

$$\eta_R\left[1-\frac{\eta_S}{\eta_R}\left(\frac{R}{S}\right)^3-\left(1-\frac{\eta_S}{\eta_R}\right)\frac{n}{n-3}\frac{\left(\frac{S}{R}\right)^{n-3}-1}{\left(\frac{S}{R}\right)^n-1}\right]$$

$$\sim\frac{3}{3-n}\eta_R-\frac{n}{3-n}\eta_S \quad (10)$$

(When $n=0$, the last two fractions in the square brackets should be replaced by $(1-R^3/S^3)/\ln(S^3/R^3)$.) When the gas volume fraction is low ($R^3/S^3\ll 1$), the effective viscosity may be further simplified, as shown in the last term of Eq. 10. For $\eta_R\gg\eta_S$ and realistic values of $n$ ($1>n>-10$), the effective viscosity is above one quarter of $\eta_R$, even if $\eta_S$ is practically zero. Thus the viscosity at the bubble–melt interface (Fig. 2a) dictates the effective viscosity. To demonstrate the importance of this effect, we compare the effective viscosity with the viscosity averaged over the volume of the melt shell (recall that $\eta_{ave}=3/(S^3-R^3)\int_R^S\eta(r)r^2dr$):

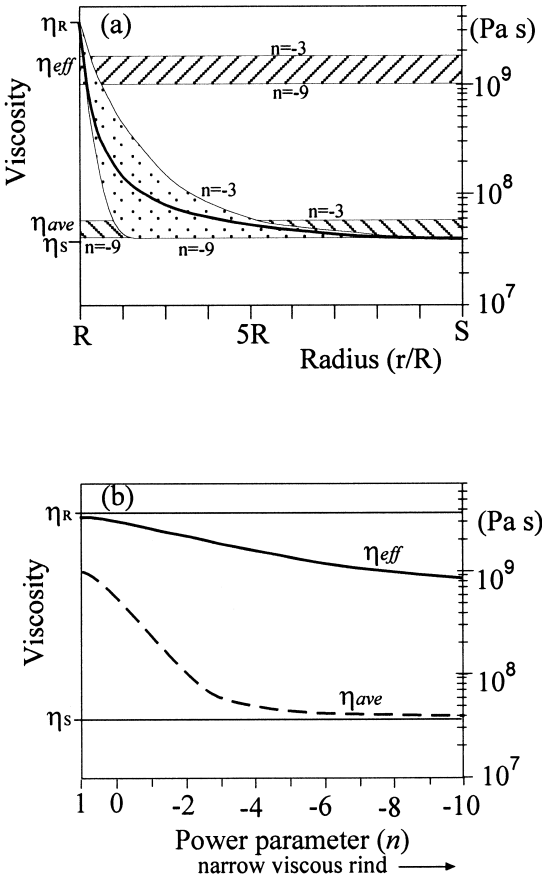


Fig. 2. (a) Radial viscosity profiles, effective viscosity, and average viscosity. The radial viscosity profile (thick curve) is obtained by combining the quasi-static water concentration profile [13], where water concentration is $C_R = 0.1$ wt% at the bubble–melt interface and $C_S = 0.6$ wt% at the shell's outer boundary, with the dependence of viscosity on water concentration [12] at 850°C. This profile is bounded (dotted area) by the polynomial approximation (Eq. 9) with power parameter $n$ between $-3$ and $-9$. The effective viscosity of the melt shell (Eq. 10) is close to $\eta_R$ (area with left-inclined stripes), whereas the average viscosity (Eq. 11) is lower by more than an order of magnitude and is closer to $\eta_S$ (right-inclined striped area). Although the average viscosity is low, the viscous resistance of the melt to gas overpressure is governed by the effective viscosity, which is very high ($>10^9$ Pa s). This means that in fast-ascending magmas, bubbles have no time to expand [16], gas pressure builds up and magma may fragment. Note that the values of both $\eta_{eff}$ and $\eta_{ave}$ are relatively restricted despite the large range of $n$. (b) The effective viscosity (thick solid curve) is typically closer to the higher-viscosity $\eta_R$ even for a thin viscous rind (small $n$), whereas the average viscosity over the volume of the shell (dashed curve) is closer to $\eta_S$ as the viscous rind narrows.

$$\eta_{ave} = \eta_R \left\{ 1 + \left(1 - \frac{\eta_S}{\eta_R}\right) \left[ \frac{\left(\frac{R}{S}\right)^n}{1 - \left(\frac{R}{S}\right)^n} \left( 1 - \frac{\frac{3}{n+3}\left(\left(\frac{S}{R}\right)^{n+3} - 1\right)}{\left(\frac{S}{R}\right)^3 - 1} \right) \right] \right\} \quad (11)$$

(When $n = -3$, the numerator in the last term should be replaced by $\ln(S^3/R^3)$ and when $n = 0$, the expression in the square brackets is replaced by $-1/\ln(R^3/S^3) - 1/(1 - R^3/S^3)$.) Fig. 2b shows that while the average viscosity is close to $\eta_S$, the effective viscosity is higher by more than an order of magnitude and is close to $\eta_R$ for a wide range of $n$ values, even for narrow viscous rinds (small $n$). Thus, the highly viscous rind around the bubble governs the effective viscosity that resists bubble growth. The consequences of high effective viscosity are discussed below.

## 4. Delayed degassing, gas overpressure, and fragmentation of rising magma

During a volcanic eruption, as hydrated magma ascends in the conduit, it becomes oversaturated and consequently degasses by growing bubbles. Along most of the ascent, melt degasses efficiently [15], so that water content in the melt is close to equilibrium with the ambient pressure. At some stage, the viscosity of the degassed melt [12] is high enough to keep gas overpressure. In this stage, the ambient pressure is low and the dependence of solubility on pressure [14] dictates faster buildup of supersaturation. This and the increase in ascent velocity towards the Earth's surface [8] lead to formation of concentration gradients and viscosity profiles that resist gas overpressure. We have shown that the effective viscosity (Eq. 8) resisting gas overpressure is approximately the viscosity at the dehydrated bubble–melt interface

and may be much higher than the average melt viscosity ($\eta_R \approx \eta_{eff} \gg \eta_{ave}$). For example, a rhyolitic melt with 0.6 wt% water that decompresses from 2 MPa to atmospheric pressure develops an effective viscosity higher than $10^9$ Pa s whereas the average viscosity is lower by more than an order of magnitude (Fig. 2). In this case, gas overpressure is preserved for time of the order of $\eta/(P_{gas}-P_{amb})$ which is longer than 500 s. An estimation of this time using the average viscosity of the melt ($5\times10^7$ Pa s) yields relaxation of gas pressure after about 20 s. In explosive volcanic eruptions, velocities in the few hundred meters before fragmentation are commonly up to 5 m/s [16]. In such cases, as the time scale for ascent is of the order of hundreds of seconds, overpressure in bubbles does not relax during the ascent of magma. If the average viscosity is used to estimate relaxation time instead of effective viscosity, one may wrongly conclude that overpressure does relax during the ascent (which means that conditions for fragmentation may not be reached).

Note that measured water content in eruption products yields information on the average melt viscosity. Additional information about the concentration profiles is needed for estimating the effective viscosity that controlled the evolution of the ejecta.

The higher effective viscosity has the following effects:

1. *Slower degassing*. Higher gas pressures and correspondingly higher water concentration at the bubble–melt interface lower the concentration gradient and limit the rate of diffusive volatile transfer into the bubble. This allows supersaturated magmas to ascend in the conduit and degas more violently at lower pressures.
2. *Bubbles maintain gas overpressure for longer times*. Magma fragments when the difference between gas pressure and ambient pressure exceeds the strength of the melt. It was recently suggested [17] that fragmentation may be triggered by a rarefaction wave. Higher effective viscosity and thus higher gas pressure in the bubbles may initiate fragmentation following weaker rarefaction, relative to previous estimations.
3. *Magma resistance to shear flow*. The relation between viscous stresses and surface tension stresses determines the resistance of bubble-bearing magma to shear flow [18,19]. During shearing of viscous magma, the higher-viscosity rinds around the bubbles will deform much less than melt of uniform viscosity, and thus will act as rigid spheres that increase the resistance of the magma to shear flow.

## 5. Conclusions

1. The effective viscosity resisting gas overpressure in the bubbles is close to the local viscosity at the dehydrated rind (Fig. 2). Thus calculations of bubble growth can include the effect of viscosity variation by simply using the above approximation without the need of evaluating Eq. 8.
2. Measured water content in eruption products yields information on the average melt viscosity. Additional information about the concentration profiles is needed for estimating the effective viscosity that controls the evolution of the ejecta.
3. High-viscosity rinds around growing water bubbles maintain gas overpressures for a longer time. This, in turn, increases the probability of fragmentation and explosive eruption.
4. The resistance of magma to shear flow in a conduit increases with the appearance of gas bubbles surrounded by a viscid dehydrated rind.

## Acknowledgements

Discussions with Alex Proussevitch and reviews by Don Dingwell and Oleg Melnik are greatly acknowledged. The project is supported by the Israel-US Binational Science Foundation. N.L. acknowledges partial support by the Yeshaya Horowitz Fellowship.*[AH]*

## References


[1] N.L. Bowen, Viscosity data for silicic melts, in: Transactions of the A.G.U. 15th Annual Meeting, 1934, pp. 249–255.

[2] Y. Zhang, A criterion for the fragmentation of bubbly magma based on brittle failure theory, Nature 402 (1999) 648–650.

[3] J.E. Mungall, N.S. Bagdassarov, C. Romano, D.B. Dingwell, Numerical modelling of stress generation and microfracturing of vesicle walls in glassy rocks, J. Volcanol. Geotherm. Res. 73 (1996) 33–46.

[4] M. Alidibirov, D.B. Dingwell, Magma fragmentation by rapid decompression, Nature 380 (1996) 146–148.

[5] P. Papale, Strain-induced magma fragmentation in explosive eruptions, Nature 397 (1999) 428.

[6] D.B. Dingwell, S.L. Webb, Relaxation of silicate melts, Eur. J. Mineral. 2 (1990) 427–449.

[7] R.S.J. Sparks, The dynamics of bubble formation and growth in magmas: a review and analysis, J. Volcanol. Geotherm. Res. 3 (1978) 1–37.

[8] L. Wilson, R.S.J. Sparks, G.P.L. Walker, Explosive volcanic eruptions. IV. The control of magma properties and conduit geometry on eruption column behavior, Geophys. J. Astron. Soc. 63 (1980) 117–148.

[9] O. Navon, A. Chekhmir, V. Lyakhovsky, Bubble growth in highly viscous melts: theory, experiments, and autoexplosivity of dome lavas, Earth Planet. Sci. Lett. 160 (1998) 763–776.

[10] A.A. Proussevitch, D.L. Sahagian, Dynamics and energetics of bubble growth in magmas: Analytical formulation and numerical modeling, J. Geophys. Res. 103 (1998) 18,223–18,251.

[11] L.D. Landau, E.M. Lifshitz, Fluid Mechanics, Addison-Wesley, Reading, MA, 1959, 536 pp.

[12] K.U. Hess, D.B. Dingwell, Viscosities of hydrous leucogranitic melts: A non-Arrhenian model, Am. Mineral. 81 (1996) 1297–1300.

[13] V. Lyakhovsky, S. Hurwitz, O. Navon, Bubble growth in rhyolitic melts: Experimental and numerical investigation, Bull. Volcanol. 58 (1996) 19–32.

[14] Y. Zhang, $H_2O$ in rhyolitic glasses and melts: measurements, speciation, solubility and diffusion, Rev. Geophys. 37 (1999) 493–516.

[15] O. Navon, V. Lyakhovsky, Vesiculation processes in silicic magmas, in: J.S. Gilbert, R.S.J. Sparks (Eds.), The Physics of Explosive Volcanic Eruptions, Geol. Soc. London Spec. Publ. 145 (1998) 27–50.

[16] R.S.J. Sparks, J. Barclay, C. Jaupart, H.M. Mader, J.C. Phillips, Physical aspects in magma degassing. I. Experimental and theoretical constraints on vesiculation, Rev. Mineral. 30 (1994) 413–445.

[17] O.E. Melnik, Dynamics of two-phase conduit flow of high-viscosity gas-saturated magma: Large variations of sustained explosive eruption intensity, Bull. Volcanol. 62 (2000) 153–170.

[18] M. Manga, J. Castro, K.V. Cashman, M. Lowenberg, Rheology of bubble bearing magma, J. Volcanol. Geotherm. Res. 87 (1998) 15–28.

[19] F.J. Spera, D.J. Stein, Comment on 'Rheology of bubble-bearing magmas' by Lejeune et al., Earth Planet. Sci. Lett. 175 (2000) 327–331.